The Journal of Immunology

ZBTB32 Restricts the Duration of Memory B Cell Recall Responses

Arijita Jash, Yinan Wang, Florian J. Weisel, Christopher D. Scharer, Jeremy M. Boss, Mark J. Shlomchik and Deepta Bhattacharya

J Immunol 2016; 197:1159-1168; Prepublished online 29 June 2016;
doi: 10.4049/jimmunol.1600882
http://www.jimmunol.org/content/197/4/1159

The Journal of Immunology is published twice each month by
The American Association of Immunologists, Inc.,
9650 Rockville Pike, Bethesda, MD 20814-3994.

Print ISSN: 0022-1767 Online ISSN: 1550-6606.

ZBTB32 Restricts the Duration of Memory B Cell Recall Responses

Arijita Jash,* Yinan Wang,*,[1] Florian J. Weisel,[†] Christopher D. Scharer,[‡,§] Jeremy M. Boss,[‡,§] Mark J. Shlomchik,[†] and Deepta Bhattacharya*

Memory B cell responses are more rapid and of greater magnitude than are primary Ab responses. The mechanisms by which these secondary responses are eventually attenuated remain unknown. We demonstrate that the transcription factor ZBTB32 limits the rapidity and duration of Ab recall responses. ZBTB32 is highly expressed by mouse and human memory B cells but not by their naive counterparts. *Zbtb32*$^{-/-}$ mice mount normal primary Ab responses to T-dependent Ags. However, *Zbtb32*$^{-/-}$ memory B cell–mediated recall responses occur more rapidly and persist longer than do control responses. Microarray analyses demonstrate that *Zbtb32*$^{-/-}$ secondary bone marrow plasma cells display elevated expression of genes that promote cell cycle progression and mitochondrial function relative to wild-type controls. BrdU labeling and adoptive transfer experiments confirm more rapid production and a cell-intrinsic survival advantage of *Zbtb32*$^{-/-}$ secondary plasma cells relative to wild-type counterparts. ZBTB32 is therefore a novel negative regulator of Ab recall responses. *The Journal of Immunology*, 2016, 197: 1159–1168.

After clearance of infection or vaccination, Ag-specific long-lived plasma cells and memory B cells persist to mediate distinct aspects of long-term humoral immunity (1). Long-lived plasma cells constitutively secrete enormous quantities of Abs irrespective of the presence of Ag (2, 3). In contrast, memory B cells secrete Abs only when they are re-exposed to cognate Ags, after which they generate more rapid and robust responses than do their naive precursors (4). Differences between primary and secondary responses are mediated by several factors. First, the precursor frequency of Ag-specific memory B cells is greater than that of their naive counterparts (5). By expanding a larger number of clones, recall responses generate more plasma cells and Ab production than in primary responses. Second, unique cell-intrinsic properties mediate the rapid expansion and differentiation of memory B cells into plasma cells. For example, Ag engagement of isotype-switched IgG, expressed by many memory B cells, leads to more robust plasma cell differentiation in vivo than does IgM signaling (6–10). Consistent with these findings, upon reactivation, IgG-expressing memory B cells robustly generate plasma cells but yield comparatively fewer germinal center B cells (5, 11, 12). Additional transcriptional mechanisms mediate rapid plasma cell differentiation by memory B cells irrespective of Ab isotype (13). As one example, mouse CD80^{+} memory B cells express low levels of the transcription factor BACH2, which otherwise inhibits plasma cell differentiation (14). Although the rapid production of Abs by memory B cells upon re-exposure to pathogens such as influenza viruses is advantageous (15), mechanisms must exist to attenuate this response once the immunogen is cleared. Given the intrinsic gene expression differences between naive and memory B cells (16–18), it is possible that unique transcriptional programs curtail secondary Ab responses.

We and others (19, 20) recently demonstrated that ZBTB20, a member of the BTB/POZ transcription factor family, promotes durable primary Ab responses when alum is used as the adjuvant. Members of this family contain an N-terminal BTB/POZ domain that mediates dimerization and recruitment of transcriptional repressors and a C-terminal domain with a variable number of zinc fingers that mediate DNA binding (21). Hallmark members of this family that regulate aspects of the immune system include BCL6, which controls germinal center and T follicular helper cell development (22–27), ThPOK, which promotes CD4 versus CD8 thymocyte fate decisions (28, 29), and PLZF, which controls NKT cell development and function (30, 31). Another member of this family, ZBTB32, was initially identified through its ability to interact with testes-specific kinases, FANCC, and GATA3 (32–34), the latter of which leads to the in vitro suppression of cytokine production by CD4 T cells. ZBTB32 is essential for the proliferative burst of NK cells in vivo (35), but other reported immunological phenotypes of *Zbtb32*$^{-/-}$ mice have been relatively subtle (36, 37). Subsequent work revealed that ZBTB32 is

*Department of Pathology and Immunology, Washington University School of Medicine, St. Louis, MO 63110; [†]Department of Immunology, University of Pittsburgh School of Medicine, Pittsburgh, PA 15261; [‡]Department of Microbiology, Emory University School of Medicine, Atlanta, GA 30322; and [§]Emory Vaccine Center, Emory University School of Medicine, Atlanta, GA 30322

[1]Current address: Weill Cornell Medical College, New York, NY.

ORCIDs: 0000-0001-9613-4932 (A.J.); 0000-0002-2432-1840 (J.M.B.).

Received for publication May 20, 2016. Accepted for publication June 6, 2016.

This work was supported by National Institutes of Health Grants R01AI099108 (to D.B.) and R01AI043603 (to M.J.S.). This work was also supported by New York Stem Cell Foundation and Research Scholar Grant 125091-RSG-13-252-01-LIB from the American Cancer Society (to D.B.). D.B. is a New York Stem Cell Foundation-Robertson Investigator. Y.W. was supported by a predoctoral fellowship from the Siteman Cancer Center. F.J.W. was supported by Deutsche Forschungsgemeinschaft Research Fellowship WE 4752/1-1. RNA-sequencing and microarray experiments were performed by the Genome Technology Access Center at Washington University, supported by National Institutes of Health Grants P30CA91842 (Siteman Cancer Center) and UL1TR000448 (Institute for Clinical and Translational Science/Clinical and Translational Science Awards).

The microarray data presented in this article have been submitted to the Gene Expression Omnibus under accession number GSE83194. The RNA-sequencing data presented in this article have been submitted to the Gene Expression Omnibus under accession number GSE81443.

Address correspondence and reprint requests to Dr. Deepta Bhattacharya, 4940 Parkview Place, Campus Box 8118, Department of Pathology and Immunology, Washington University School of Medicine, St. Louis, MO 63110. E-mail address: deeptab@pathology.wustl.edu

The online version of this article contains supplemental material.

Abbreviations used in this article: CGG, chicken gammaglobulin; NP, 4-hydroxy-3-nitrophenyl-acetyl.

highly induced in B cells by LPS stimulation, partially represses *Ciita* transcripts, and is preferentially expressed by the $CD80^+$ subset of memory B cells (13, 38). Yet the functional consequences of ZBTB32 expression in the B cell lineage are uncertain. In this study, we demonstrate that ZBTB32 specifically limits the rapidity and duration of memory B cell–mediated recall responses.

Materials and Methods

Mice

All animal procedures were approved by the Animal Studies Committee at Washington University in St. Louis (approval number 20140030). C57BL/6N, B6.SJL*Ptprc*^{a}*Pepc*^{b} (B6.SJL) and B6.Cg*Igh*^{a}*Thy1*^{a}*Gpi1*^{a} (*IgH*^{a}) mice were purchased from Charles River Laboratories. *Zbtb32*$^{-/-}$ mice have been described previously (36). All mice were bred in the animal facilities of the Washington University School of Medicine under pathogen-free conditions and experiments were performed in compliance with Washington University Animal Studies guidelines.

RNA extraction, cDNA synthesis and quantitative RT-PCR

Total RNA was extracted with TRIzol (Life technologies) and first strand cDNA synthesis was performed with Superscript III Reverse transcription kit using oligo (dT) primers or random hexamers (Life Technologies) according to the manufacturer's instructions. Quantitative RT-PCR was performed using SYBR Green PCR master mix (Applied Biosystems) on a Prism 7000 Sequence Detection System (Applied Biosystems). The primer sequences are as follows: Zbtb32, 5′-GGTGCTCCCTTCTCCCATAGT-3′ (forward) and 5′-GGAGTGGTTCAAGGTCAGTG-3′ (reverse); β-actin, 5′-CCTGAACCCTAAGGCCAAC-3′ (forward) and 5′-ACAGCCTGG-ATGGCTACG-3′ (reverse).

Immunization and adoptive transfer for recall responses

Zbtb32$^{+/+}$ and *Zbtb32*$^{-/-}$ mice 8–10 wk of age were immunized i.p. with a single dose of 100 μg of 4-hydroxy-3-nitrophenyl-acetyl–chicken gammaglobulin (NP-CGG; hapten protein ratio: 15–22; Biosearch Technologies) precipitated in 5% aluminum potassium sulfate (Thermo Fisher Scientific) in PBS. Spleens were harvested 8–10 wk post immunization, and single-cell suspensions of splenocytes were subjected to gradient centrifugation using Histopaque 119 (Sigma-Aldrich) for 10 min at 2000 × *g* to remove the noncellular debris. Interface cells were then collected, and RBCs were lysed by resuspending in buffer containing 0.15 M NH_4Cl, 10 mM $KHCO_3$, and 0.1 mM EDTA (pH 7.2). Cells were washed twice with PBS, and 10% of the cells were retained for flow cytometric analysis. The remaining splenocytes were adoptively transferred into one, two, or three nonirradiated *IgH*^{a}- or B6.SJL-recipient mice, as described in each figure, by i.v. injection. A recall response was then elicited in the recipient mice 24 h later by i.v. administration of 50 μg of soluble NP-CGG.

Serological analysis

ELISA plates were coated overnight at 4°C with 5 μg/ml NP_{16}BSA, NP_4BSA, or CGG (Biosearch Technologies) in bicarbonate coating buffer (0.1 M sodium bicarbonate and 0.02% sodium azide at pH 9.6). Plates were washed with wash buffer (PBS containing 0.05% Tween 20), and after blocking 1 h with blocking buffer (PBS supplemented with 2% BSA and 0.05% Tween 20) at 37°C, serially diluted serum samples were added and incubated for 1 h at room temperature. Technical duplicates were performed for every serum sample. Plates were washed with PBS with 0.05% Tween 20 and incubated with 1 μg/ml biotinylated anti-$IgG1^b$ (B682; BD Biosciences) for 1 h, followed by streptavidin-conjugated HRP for 45 min. Peroxidase activity was detected by tetramethylbenzidine substrate (DakoCytomation), and the reaction was quenched with 2 N H_2SO_4, and ODs were quantified at 450 nm. The end-point titer of each sample was determined using Prism software (GraphPad Software) from a one phase exponential decay curve defined as the dilution that generates an OD_{450} value of the background plus 3 SDs.

ELISPOT assays

For the detection of NP-specific Ab-secreting cells, MultiScreen filter plates (EMD Millipore) were coated with 50 μg/ml NP_{16}BSA in PBS overnight. Total bone marrow cells were harvested 9 wk after recall from *IgH*^{a}-recipient mice and were seeded at 5–10 × 10^6 cells/well in technical triplicates for every sample. Cells were cultured in 100 μl of RPMI 1640 medium/5% FBS overnight at 37°C. Wells were washed with PBS containing 0.05% Tween 20 and stained with biotinylated anti-$IgG1^b$ and streptavidin-conjugated HRP (BD Biosciences). Spots were developed with 3-amino 8-ethyl carbazole (Sigma-Aldrich), and the reaction was stopped by rinsing the plates with water and the spots were counted in ImmunoSpot S6 Analyzer (CTL Laboratories).

Abs

The following mAbs were purified from hybridoma supernatants by BioXCell: 2C11 (anti-CD3), GK1.5 (anti-CD4), 536.7 (anti-CD8), 1D3 (anti-CD19), 8C5 (anti-Gr1), M1/70 (CD11b), TER119 (anti-Ter119), A20.1.7 (anti-CD45.1). Purified Abs were conjugated to Pacific Blue or Alexa Fluor 680 (Life Technologies), according to the manufacturer's instructions. The following Abs were purchased from eBioscience: II/41 (anti-IgM)-PerCP–eFluor 710 or FITC, 1126 (anti-IgD)-FITC or Qdot 605, and GL-7 conjugated to biotin. The following Abs were purchased from BioLegend: A-20 (CD45.1)-allophycocyanin-Cy7, 1610A1 (anti-CD80)-PE, 29-2L17 (anti-CCR6)-PeCy7, GL-7-Pacific Blue, RA3-6B2 (B220)-Alexa 488 or -PerCp-Cy5.5, 281-2 (CD138)-PE or -allophycocyanin, ICRF44 (CD11b)-PerCp-Cy5.5, 104D2 (CD117)-PerCp-Cy5.5, RB68C5 (Ly6G)-BV605, anti-human CD20 (2H7)-allophycocyanin-Cy7, anti-human CD27 (O323)-Alexa 647, anti-human CD38 (HIT2)-PE-Cy7, anti-human CD2 (RPA-2.10)-PE, anti-human CD19 (HIB2)-BV421, anti-human IgM (MHM-88)-FITC, anti-human CD138 (MI15)-FITC, and streptavidin-Qdot 605. Unlabeled Mouse anti rat IgG (H+L) was bought from Southern Biotechnology Associates. NP–allophycocyanin used for surface staining and in intracellular staining was made by conjugating allophycocyanin (Sigma-Aldrich) with NP-O–succinimide ester (Biosearch Technologies) as described previously (39, 40).

Cell isolation, analysis, and purification

Bone marrow plasma cells were sorted following CD138 enrichment in which total bone marrow cells were stained with 1 μl of anti–CD138-PE (BioLegend) for every 10^7 cells. $CD138^+$ cells were selectively enriched using anti-PE magnetic beads (4 μl of beads /10^7 cells) and MACS LS columns (Miltenyi Biotec) prior to flow cytometric analysis and/or purification. Total splenocytes were depleted of the non-B cell lineage cells and IgM^+, IgD^+, and $GL\text{-}7^+$ cells by cellular panning. Briefly, cells were surface stained with rat anti-mouse Abs against non-B cell lineage cells (CD3, CD4, CD8, Gr1, CD11b, and Ter119), non–class-switched (IgM^+, IgD^+), and germinal center B ($GL\text{-}7^+$) B cells for 30 min on ice. Cells were then washed with and incubated in plates precoated with 1 μg/ml mouse anti rat IgG (Southern Biotechnology Associates) for 30 min at 4°C. The nonadherent cell fraction was then collected, washed, and stained to identify the resting and NP^+ memory B cells ($CD19^+CCR6^+CD80^+$ class-switched IgM^-IgD^- cells). For microarrays, resting memory B cells and donor (CD45.2)-derived NP-specific activated memory B cells and bone marrow plasma cells were sorted into PBS with 5% FBS or directly into RNA lysis buffer (Macherey–Nagel). All cell analysis and sorting was done on a FACS Aria II (BD Biosciences).

BrdU labeling and analysis

Following adoptive transfer and NP-CGG rechallenge, mice were fed with 2 mg/ml BrdU in the drinking water for the durations indicated. Splenic plasma cells, memory B cells and CD138-enriched bone marrow plasma cells were first stained for surface expression of respective Abs as described in Supplemental Fig. 1. Cells were then processed and stained for incorporated BrdU with the FITC BrdU Flow kit (BD Biosciences), according to the manufacturer's instructions.

Microarrays and analysis

Total RNA was prepared from purified resting memory B cells (5,000–10,000 cells), donor-derived NP-specific day 7 memory B cells (100–500 cells), and donor-derived NP-specific bone marrow plasma cells (100–500 cells) using a NucleoSpin RNA isolation kit (Macherey–Nagel), which includes a DNase digestion step. cDNA amplification using the GeneChip WT Pico Kit and hybridization of labeled cDNA to GeneChip Mouse Gene 1.0 ST Arrays (Affymetrix) were performed by the Genome Technology Access Center core facility at Washington University in St. Louis. Analysis of microarray data was performed using Arraystar software (DNASTAR). Quantiles-based normalization was performed, and Student two-tailed *t* tests were used to calculate differentially expressed genes with $p < 0.05$ without multiple test correction. All such differentially expressed genes were entered into the Consensus Pathway Database (http://cpdb.molgen.mpg.de/), and enriched pathways with $q < 0.05$ were considered significant. Data can be accessed through the National Center for Biotechnology Information Gene Expression Omnibus database under accession number GSE83194 (http://www.ncbi.nlm.nih.gov/geo/query/acc.cgi?acc=GSE83194).

Human tissues

All procedures in this study were approved by the Human Research Protection Office at Washington University. Bone marrow was obtained from

total hip arthroplasty samples from patients undergoing elective surgery (Barnes Jewish Hospital). For bone marrow aspirates, 20–30 ml of IMDM was added, samples were dissociated using vigorous agitation, and filtered through 70-μM nylon mesh. RBCs were removed using 0.15 M NH_4Cl, 10 mM $KHCO_3$, and 0.1 mM EDTA (pH 7.2) buffer, samples were stained with 1 μl/10^7 cells anti-CD138 microbeads (Miltenyi Biotec), and enriched on an AutoMacs machine (Miltenyi Biotec) over two columns. Peripheral blood was obtained from the Barnes Jewish Hospital Pheresis center from waste Trima fillers. Samples were spun through a 1.077 g/ml Histopaque gradient (Sigma-Aldrich), interface cells were collected, lysed with 0.15 M NH_4Cl, 10 mM $KHCO_3$, and 0.1 mM EDTA (pH 7.2), and stained for FACS as in Supplemental Fig. 1.

RNA sequencing and analysis

Human samples gated as shown in Supplemental Fig. 1 were double-sorted into RLT buffer (Qiagen), and RNA was prepared using an RNeasy Micro kit (Qiagen). Sequencing libraries were generated using a Clontech Smart-Seq kit. Single-end 50-bp reads were acquired using an Illumina HiSEquation 2500. Reads were mapped to the Ensembl_R72 reference human genome using Tophat (https://usegalaxy.org/). Resultant .bam files were processed, and reads per kb of transcript per million mapped read values were computed using Partek software. Data can be accessed through the National Center for Biotechnology Information Gene Expression Omnibus database under accession number GSE81443 (http://www.ncbi.nlm.nih.gov/geo/query/acc.cgi?acc=GSE81443).

Statistics

Means, geometric means, SEM, 95% confidence interval, unpaired Student 2-tailed *t* tests, Mann–Whitney tests, and one-phase exponential decay curve fitting for end-point dilution estimation were calculated with Prism software.

Results

ZBTB32 is highly expressed in mouse and human memory B cells

ZBTB32 is highly expressed by $CD80^+PD\text{-}L2^+$ memory B cells (13), independent of whether they express IgM or IgG. These cells preferentially differentiate into plasma cells instead of germinal center B cells upon antigenic rechallenge (13). To expand the analysis to other B cell subsets (Supplemental Fig. 1), we performed quantitative RT-PCR analysis. Mouse polyclonal $CD80^+$ memory B cells express 20- to 30-fold higher levels of ZBTB32 transcripts than do naive and germinal center B cells and polyclonal bone marrow plasma cells (Fig. 1A). RNA-seq analysis of human lineages also revealed expression of ZBTB32 in both IgM^+ and IgG^+ memory B cells but undetectable expression in naive B cells and polyclonal bone marrow plasma cells (Fig. 1B). Thus, ZBTB32 is specifically expressed by both mouse and human memory B cells.

ZBTB32 deficiency prolongs secondary but not primary Ab responses

We next performed experiments to define the functional role of ZBTB32 in primary and secondary Ab responses. *Zbtb32*$^{-/-}$ mice were immunized with the T-dependent Ag NP-CGG, and Ag-specific serum Ab titers were quantified at 1 and 8 wk postimmunization. No differences were observed in NP-specific serum Ab titers between *Zbtb32*$^{+/+}$ and *Zbtb32*$^{-/-}$ mice at either time point (Fig. 2A). At 10 wk postimmunization, *Zbtb32*$^{+/+}$ and *Zbtb32*$^{-/-}$ mice possessed similar numbers of NP-specific splenic memory B cells (Fig. 2B). Moreover, the ratios of Ag-specific $CD80^+PD\text{-}L2^+$, $CD80^-PD\text{-}L2^+$, and $CD80^-PD\text{-}L2^-$ memory B cell subsets were unchanged in *Zbtb32*$^{-/-}$ mice (dat not depicted). Thus, ZBTB32 is dispensable for primary Ab responses.

To test secondary responses, splenocytes from *Zbtb32*$^{+/+}$ and *Zbtb32*$^{-/-}$ mice 10 wk after NP-CGG immunization were adoptively transferred into allotype-distinct naive IgH^a mice. One day later, these recipients were challenged i.v. with soluble NP-CGG to elicit a recall response. Donor $IgG1^b$ NP-specific serum Ab titers derived from *Zbtb32*$^{-/-}$ cells were elevated relative to controls at 1 wk postimmunization (Fig. 3A). In subsequent weeks, wild-type Ag-specific $IgG1^b$ titers gradually declined, but Abs derived from *Zbtb32*$^{-/-}$ cells remained elevated (Fig. 3A). The affinities of these Abs were similar between donor genotypes, as measured by NP_4/NP_{16} binding ratios (Fig. 3B). At 9 wk postimmunization, ELISPOT assays were performed to quantify the numbers of NP-specific Ab-secreting cells. Far greater numbers of bone marrow *Zbtb32*$^{-/-}$ $IgG1^b$ NP-specific Ab-secreting cells were observed relative to *Zbtb32*$^{+/+}$ controls (Fig. 3C). We also examined Ab titers specific for CGG because these responses qualitatively differ from those against haptens (41, 42). Although end-point titers were difficult to calculate in this response, CGG-specific Abs derived from *Zbtb32*$^{-/-}$ cells were clearly elevated relative to controls at both early and late time points (Fig. 3D). Thus, ZBTB32 restricts the rapidity and duration of Ab production following memory B cell recall responses to both haptens and proteins.

The rapid and prolonged *Zbtb32*$^{-/-}$ memory B cell recall responses could be driven by either cell-extrinsic or -intrinsic changes. These changes could manifest in memory B cells and/or their downstream plasma cells. To distinguish between these possibilities, $CD45.2^+$ *Zbtb32*$^{+/+}$ and *Zbtb32*$^{-/-}$ and $CD45.1^+$ wild-type mice were immunized with NP-CGG. At 10 wk postimmunization, $CD45.1^+$ and $CD45.2^+$ splenocytes were mixed at equal ratios and transferred into naive $CD45.1^+$ recipients (Fig. 4A). Mice were challenged with i.v. NP-CGG, and Ag-specific B cell subset chimerism was assessed 7 and 21 d later. Under these conditions, we observed almost no $CD45.2^+$ donor germinal center B cells (data not depicted). $CD45.2^+$ donor chimerism was similar between *Zbtb32*$^{+/+}$ and *Zbtb32*$^{-/-}$ bone marrow plasma cells at day 7 (Fig. 4B). However, *Zbtb32*$^{-/-}$ bone marrow plasma cell chimerism was elevated at day 21 relative to controls (Fig. 4B, Supplemental Fig. 2). A slight decrease in $CD45.2^+$ chimerism was observed be-

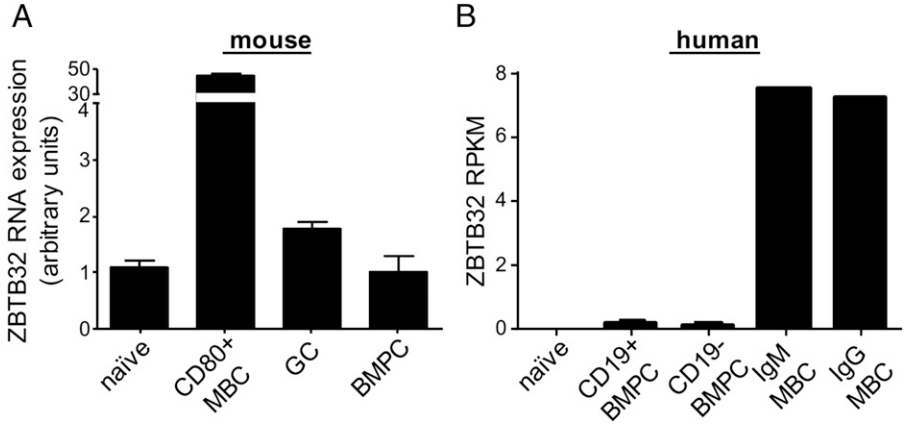

FIGURE 1. ZBTB32 is highly expressed by mouse and human memory B cells. (**A**) Transcript levels of *Zbtb32* in mouse naive, $CD80^+$ memory B cells (MBC), germinal center B cells (GC), and bone marrow plasma (BMPC) cells were measured by quantitative RT-PCR in technical triplicate. The data were normalized to the mean β-actin (Actb) expression for each sample. Mean values ± SD are shown in arbitrary units (AU). The data are representative of two independent experiments. (**B**) RNA-seq analysis of *Zbtb32* expression in human B cell subsets. Data are shown as reads per kb of transcript per million mapped reads (RPKM).

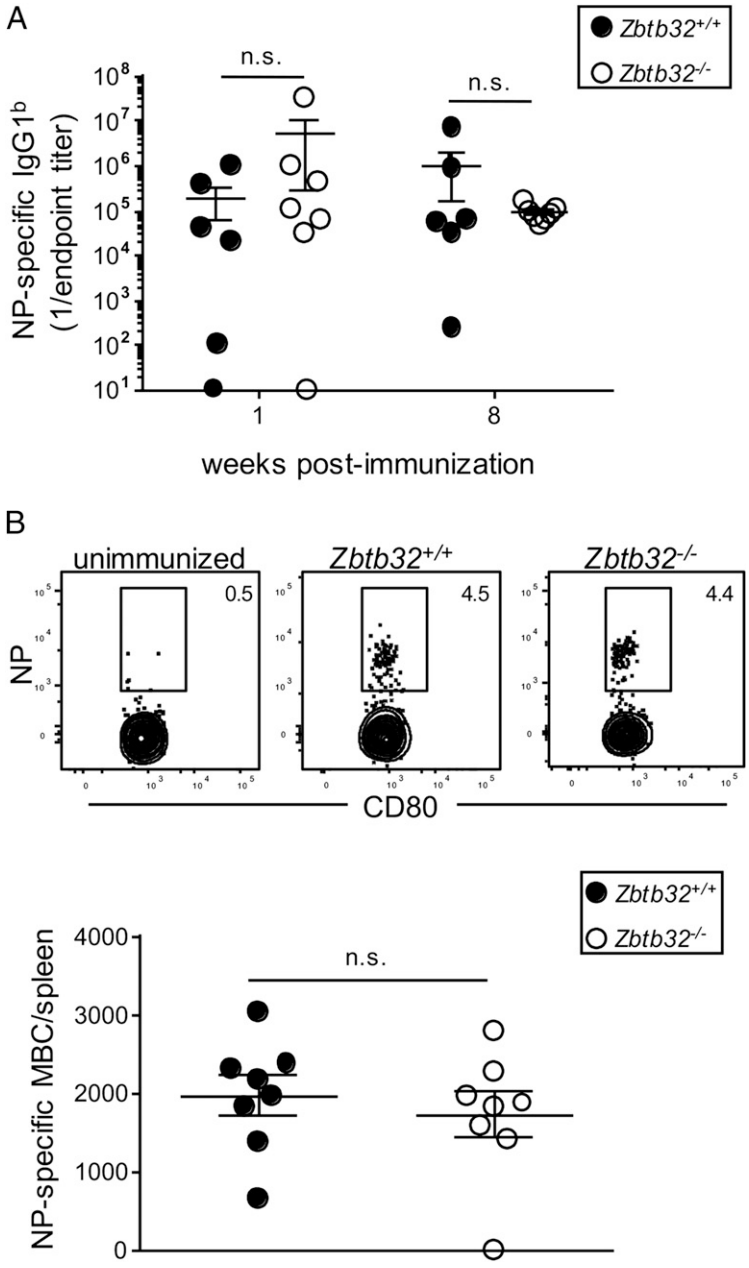

FIGURE 2. ZBTB32 is dispensable for primary Ab responses. (**A**) ELISA measurement of serum NP-specific IgG1 Abs in *Zbtb32*$^{+/+}$ and *Zbtb32*$^{-/-}$ mice. Error bars depict geometric means ± 95% confidence interval. Each dot indicates an individual mouse. Data are representative of two independent experiments and statistical significance was calculated by Mann–Whitney *U* test. $p > 0.05$. (**B**) Frequencies and absolute numbers of NP-specific *Zbtb32*$^{+/+}$ and *Zbtb32*$^{-/-}$ memory B cells 10 wk after primary immunization were quantified by flow cytometry. Mean values ± SEM are shown. Representative plots are shown in the top panels. Statistical significance was determined with an unpaired Student two-tailed *t* test.

tween days 7 and 21 in both genotypic groups (Fig. 4B), likely because of delayed host CD45.1^{+} responses to NP-CGG. No differences in chimerism were observed between *Zbtb32*$^{+/+}$ and *Zbtb32*$^{-/-}$ memory B cells at either day 7 or 21 (Fig. 4C, Supplemental Fig. 2). Similarly, splenic plasma cell chimerism was similar between *Zbtb32*$^{+/+}$ and *Zbtb32*$^{-/-}$ genotypes at day 7 (Fig. 4D, Supplemental Fig. 2). At day 21, we were unable to identify splenic Ag-specific plasma cells above background staining (data not depicted). These data demonstrate that ZBTB32 deficiency prolongs Ab responses by elevating the numbers of secondary bone marrow plasma cells at late time points through a cell-intrinsic mechanism.

Though these data provide a cellular basis for durable *Zbtb32*$^{-/-}$ Ab recall responses, they do not explain the elevated Ab levels at early timepoints (Fig. 3A). We hypothesized that ZBTB32 deficiency leads to more rapid Ab production relative to controls at timepoints before day 7 in the recall response. Because Ag-specific cells are difficult to quantify by flow cytometry at these early stages (data not depicted), we turned to a more sensitive system. *Zbtb32*$^{+/+}$ and *Zbtb32*$^{-/-}$ mice were immunized, and 8 wk later, T cell–depleted splenocytes were transferred along with wild-type T cells from NP-CGG–primed mice into *Rag1*$^{-/-}$ recipients. At 3.5 and 4.5 d posttransfer and immunization, ELISPOT assays were performed on splenocytes. At both time points, *Zbtb32*$^{-/-}$ memory B cells yielded more splenic Ab-secreting cells than did control memory cells (Fig. 4E). Taken together, these data demonstrate that ZBTB32 deficiency leads to more rapid production of secondary plasma cells in the spleen and more prolonged maintenance of secondary plasma cells in the bone marrow relative to ZBTB32-sufficient controls.

ZBTB32 deficiency leads to altered expression of cell cycle and mitochondrial translation genes in secondary plasma cells

The prolonged Ab production phenotype could be caused by ZBTB32-mediated regulation of differentiation programs in memory B cells and proliferative and/or survival programs in bone marrow plasma cells. We performed microarray analyses of *Zbtb32*$^{+/+}$ and *Zbtb32*$^{-/-}$ resting memory B cells, NP-specific activated memory B cells isolated 7 d after adoptive transfer and immunization, and

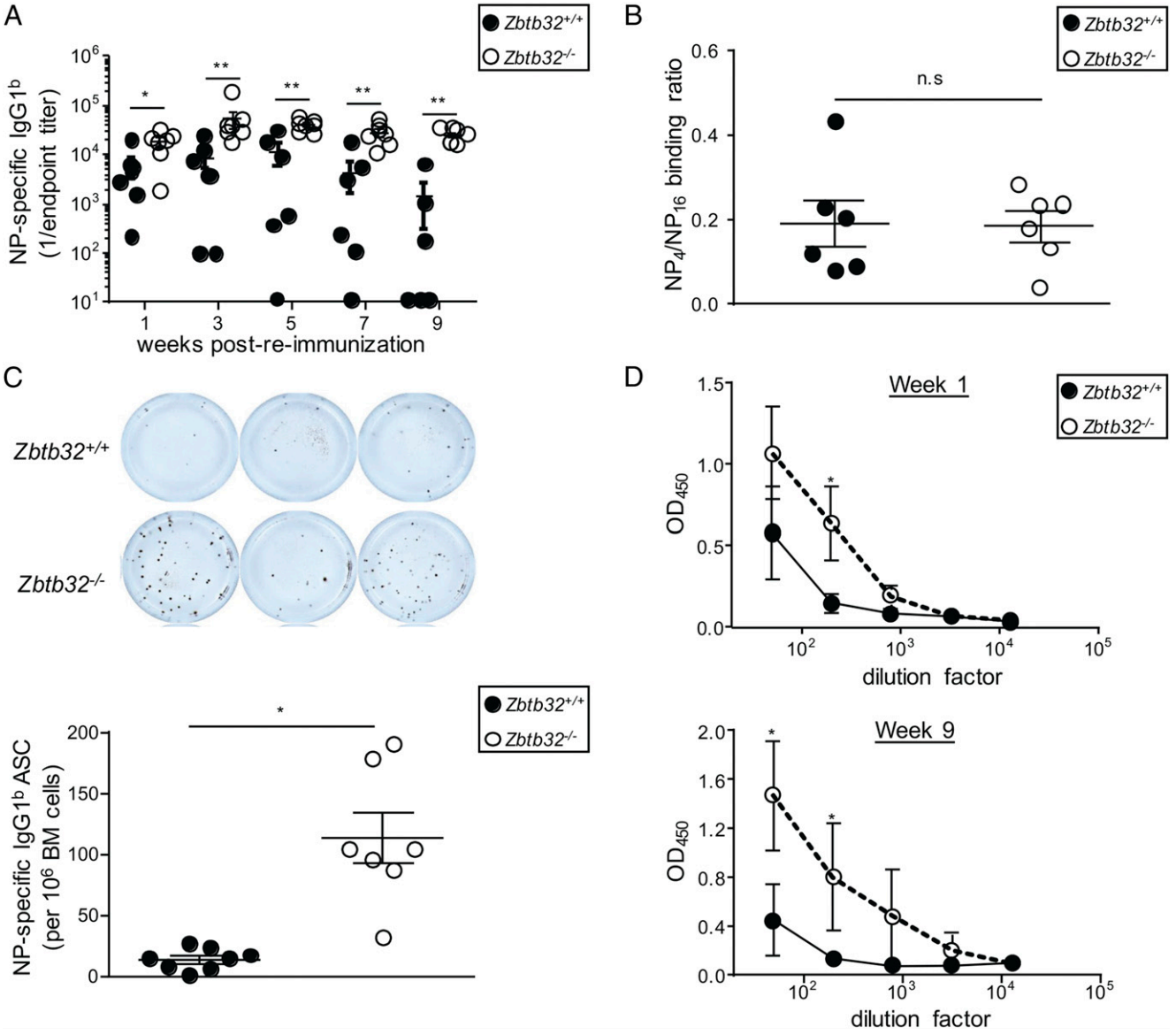

FIGURE 3. ZBTB32 deficiency sustains memory B cell recall responses. (**A**) ELISA measurement of memory B cell responses. *Zbtb32*$^{+/+}$ and *Zbtb32*$^{-/-}$ mice were immunized, and 10 wk later, splenocytes were transferred to naive *Igh*^{a} recipients. One day later, recipients were immunized i.v. with soluble NP-CGG. Donor IgG1^{b} NP–specific Abs were quantified by ELISA. Each dot represents an individual mouse. Data are representative of two independent experiments each with three to eight mice per genotype. Error bars depict geometric means ± 95% confidence interval, and statistical significance was determined by the Mann–Whitney *U* test. *$p < 0.05$, **$p < 0.01$. (**B**) ELISA measurements of relative affinity of NP-specific serum Abs generated 1 wk after recall response with soluble NP-CGG. Ratios of high-affinity (NP_4 binding) to total (NP_{16} binding) Abs were quantified, and mean values ± SEM are shown. Each dot represents an individual mouse, and the data are representative of three experiments, each with four to six mice per genotype. Statistical significance was determined by Mann–Whitney *U* test. (**C**) NP-specific Ab-secreting cells in the bone marrow of recipient mice at 9 wk post-rechallenge were enumerated by ELISPOT. Representative images (original magnification ×10) are shown in the top panels, and quantification is shown in the bottom panels. Mean values ± SEM are shown. Statistical significance was determined with an unpaired Student two-tailed *t* test. *$p < 0.05$. Each data point represents one mouse. Data are representative of two independent experiments. (**D**) ELISA measurement of memory B cell recalls responses to CGG. Background-subtracted OD values obtained at 450 nm (OD_{450}) were plotted against the serum dilutions and mean values ± SEM are shown. Each dot represents the mean of the ODs of three to six biologically distinct samples from different mice at each dilution point. Data are representative of two independent experiments. Statistical significance was determined by Student two-tailed *t* test, *$p < 0.05$.

NP-specific secondary bone marrow plasma cells at this same time point (Supplemental Fig. 3). The magnitude of gene expression differences between *Zbtb32*$^{+/+}$ and *Zbtb32*$^{-/-}$ resting memory B cells was relatively modest, with only 34 genes displaying statistically significant >2-fold expression changes (Fig. 5A). Even when all 1386 statistically significant transcripts were analyzed, no clear signatures could be derived from Consensus Pathway Database analysis (http://cpdb.molgen.mpg.de/). Upon activation in vivo, 147 genes became differentially expressed >2-fold between *Zbtb32*$^{+/+}$ and *Zbtb32*$^{-/-}$ CD80^{+} memory B cells (Fig. 5A). Pathway analysis of all statistically significant changes in *Zbtb32*$^{-/-}$ activated memory B cells revealed elevated expression of genes such as cathepsins A, B, and D, which are involved in lysosomal function and Ag processing (43), and the dual-specificity phosphatases 1, 7, and 16, which regulate MAPK signaling (44) (Fig. 5B). Yet, we observed no transcriptional evidence of changes in signatures related to proliferation or survival, consistent with the data in Fig. 4C.

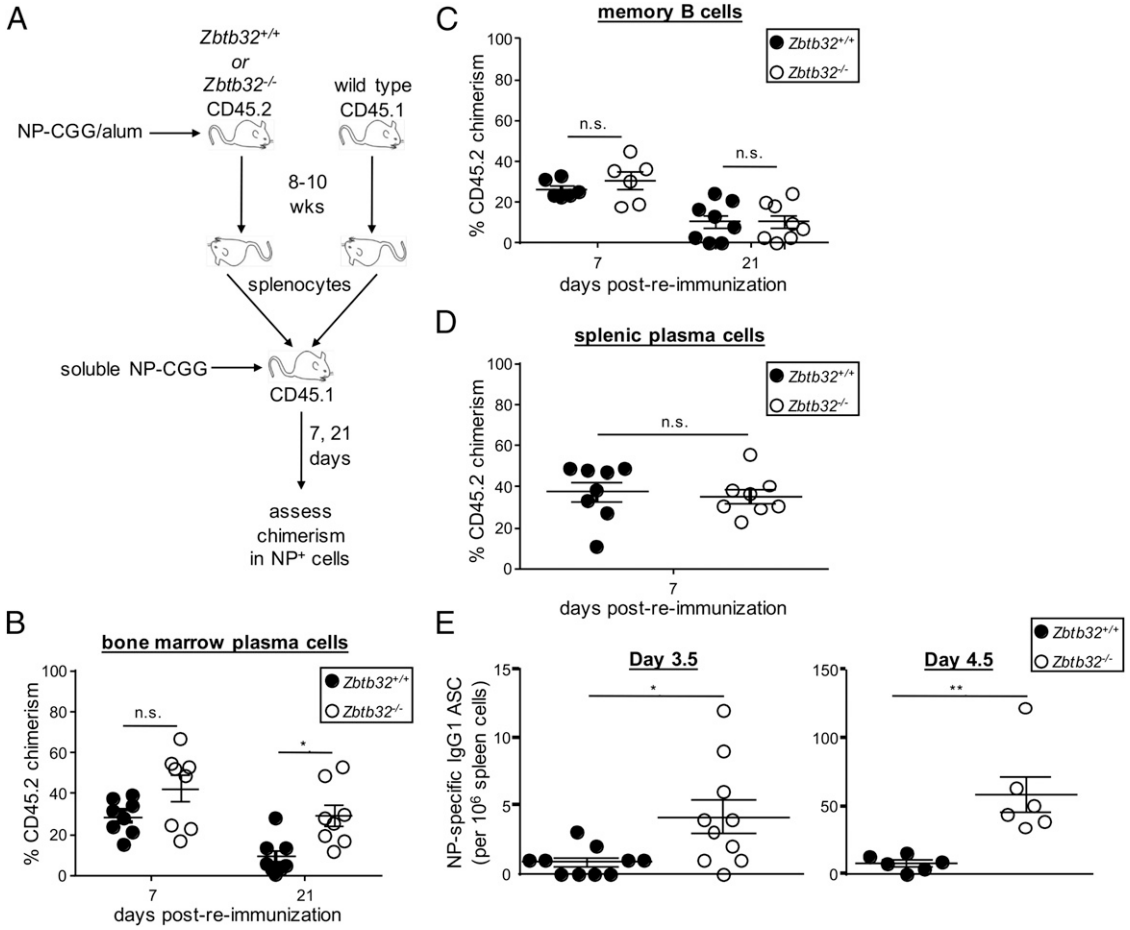

FIGURE 4. Cell-intrinsic ZBTB32 deficiency increases the number of memory B cell–derived bone marrow plasma cells. (**A**) Schematic representation of transfer experiment. Donor chimerism in NP-specific bone marrow plasma cells (**B**), memory B cells (**C**), and splenic plasma cells (**D**) were determined by flow cytometry at days 7 and 21 postimmunization. (**E**) ELISPOT analysis of early recall responses. $Zbtb32^{+/+}$ and $Zbtb32^{-/-}$ mice were immunized with NP-CGG, and at 8 wk, T cell–depleted splenocytes containing 5000 NP-specific memory B cells were transferred into $Rag1^{-/-}$ recipients alongside 8×10^5 $CD4^+$ T cells from NP-CGG–primed wild-type mice. Recipients were immunized with NP-CGG and ELISPOT assays were performed on splenocytes at 3.5 and 4.5 d postchallenge. Mean values ± SEM are shown along with individual data points. Each panel represents cumulative data from two to five experiments. Statistical significance was determined with an unpaired Student two-tailed *t* test. $*p < 0.05$.

Among secondary bone marrow plasma cells, ZBTB32 expression itself was extinguished (Fig. 5A). When all 1177 statistically significant differences were considered, $Zbtb32^{-/-}$ NP-specific secondary bone marrow plasma cells displayed elevated expression of numerous genes known to promote cell cycle progression (Fig. 5C), such as *E2f3*, which transcriptionally promotes entry into S-phase (45), and *Pcna*, which promotes DNA replication (46, 47). In addition, we observed elevated expression of numerous mitochondrial ribosomal genes (*Mrpl18*, *Mrps22*, *Mrpl51*, *Mrps25*, *Mrps30*, *Mrpl30*, and *Mprs27*), which promote translation (Fig. 5C). Mitochondrial translation is essential for production of proteins involved in the electron transport chain (48), and we have shown that maximal respiratory capacity is essential for long-lived plasma cell survival (49). Thus, the transcriptional data of bone marrow $Zbtb32^{-/-}$ secondary plasma cells suggest increased proliferation and survival, either or both of which could contribute to prolonged Ab production in vivo.

ZBTB32 deficiency promotes survival of secondary plasma cells

To distinguish between these possibilities, we performed BrdU labeling experiments. Immunizations and adoptive transfers were established, and mice were given BrdU in the drinking water for 3 d prior to analysis (Fig. 6A, Supplemental Fig. 4) (50). The majority of both $Zbtb32^{+/+}$ and $Zbtb32^{-/-}$ bone marrow plasma cells had incorporated BrdU at day 7, suggesting either recent proliferation or derivation from upstream proliferating precursors (Fig. 6B, Supplemental Fig. 4). There was a trend toward increased BrdU incorporation by $Zbtb32^{-/-}$ secondary plasma cells (Fig. 6B), perhaps reflective of the transcriptional data, elevated serum Abs at this time point, and increases in early plasma cell numbers (Figs. 3A, 4E, 5C). However, this difference did not reach statistical significance, and by day 21, we observed little BrdU incorporation in either genotypic group (Fig. 6B). The majority of splenic memory B and plasma cells also incorporated BrdU at day 7 (Fig. 6C, 6D, Supplemental Fig. 4). Splenic plasma cells were difficult to detect at day 21, but memory B cells showed little evidence of BrdU incorporation at day 21 (Fig. 6C). Thus, by day 21, proliferation had subsided in all Ag-specific B cell subsets. To further demonstrate this point, we performed BrdU pulse-chase experiments. Adoptive recipients of $Zbtb32^{+/+}$ and $Zbtb32^{-/-}$ immune splenocytes were challenged with NP-CGG and concomitantly fed BrdU in the drinking water for 7 d. Animals were then given normal drinking water for 14 d, and bone marrow plasma cells were analyzed. BrdU label retention in donor bone marrow plasma cells was similar between $Zbtb32^{+/+}$ and $Zbtb32^{-/-}$ genotypes (Fig. 6E). These data demonstrate that ZBTB32 restricts the duration of secondary Ab responses by attenuating survival, rather than the proliferation of plasma cells.

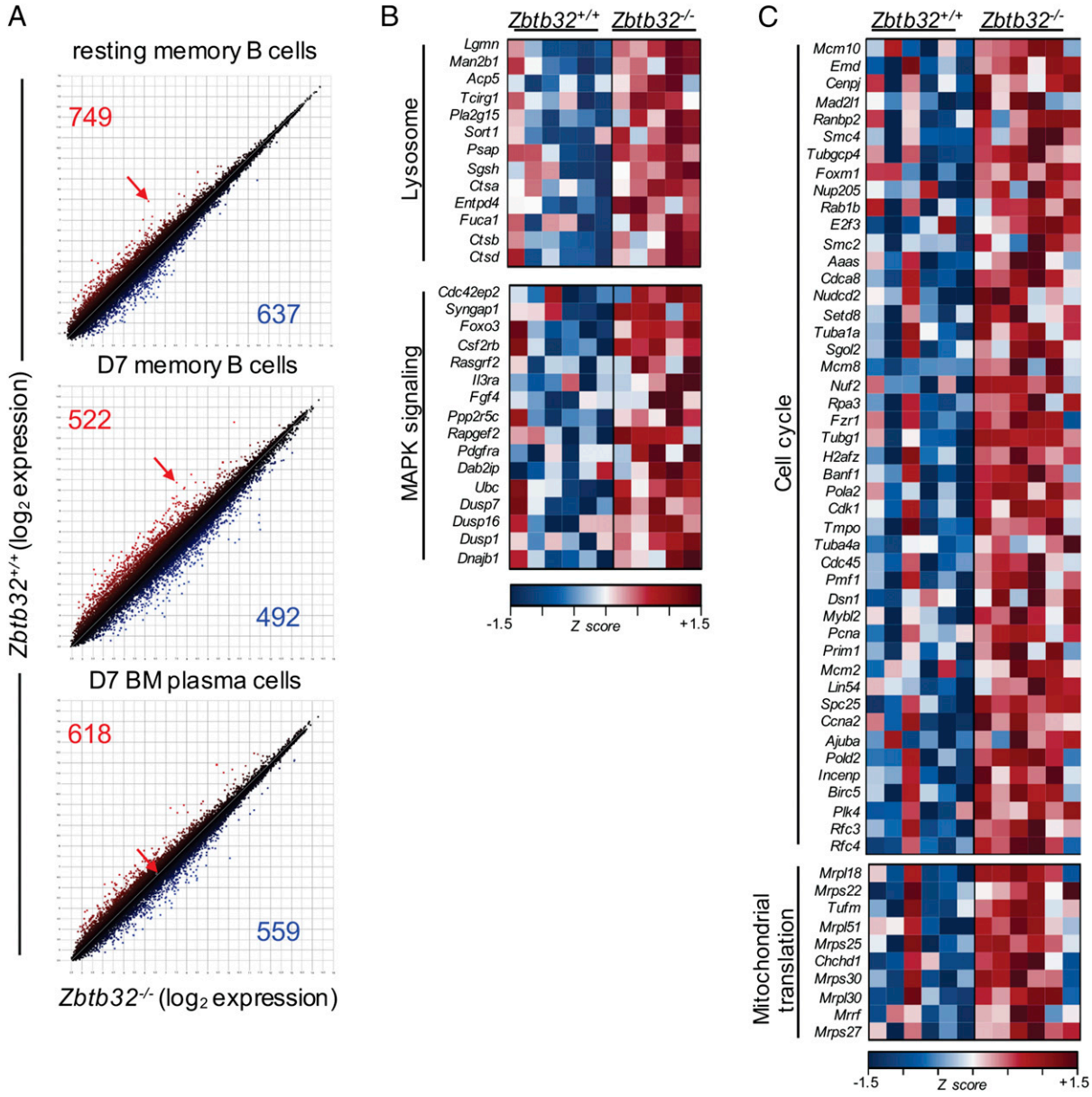

FIGURE 5. *Zbtb32*$^{-/-}$ secondary plasma cells express elevated cell cycle and mitochondrial translation genes. (**A**) Scatter plots depicting microarray analysis in *Zbtb32*$^{+/+}$ and *Zbtb32*$^{-/-}$ resting memory B cells (top panel), activated donor-derived NP-specific memory B cells at day 7 of the recall response (middle panel), and donor-derived secondary NP-specific bone marrow plasma cells at day 7 of the recall response (bottom panel). Arrows indicate the probeset specific for *Zbtb32*. Pathway enrichment analysis of all differentially expressed transcripts in day 7 NP-specific *Zbtb32*$^{-/-}$ memory B cells (**B**) or secondary bone marrow plasma cells (**C**) with q values < 0.05. Blue represents low and red represents high relative expression levels.

Discussion

In this study, we have demonstrated that the transcription factor ZBTB32 is important for attenuating Ab production after a memory B cell recall response. Given that ZBTB32 expression is turned off by the plasma cell stage, the data imply that lifespan is imprinted during the upstream activation phase, as has been previously proposed (51, 52). Yet, no molecular mechanism has yet been determined that would explain this process. In our study, we observed that activated *Zbtb32*$^{-/-}$ memory B cells elevate expression of genes involved in lysosomal and MAPK pathways. The elevated expression of lysosomal genes such as cathepsins is of particular interest, given their importance in MHC class II Ag processing (43). It is possible that upon reactivation, *Zbtb32*$^{-/-}$ memory B cells are better at presenting peptide:MHC class II and receiving T cell help than are their wild-type counterparts. Although the extreme paucity of Ag-specific memory B cells in vivo has limited our ability to test this hypothesis, this model is consistent with other studies showing that the ability to interact with T cells is a major determinant of B cell fate (53, 54). Exactly how this interaction would promote longevity in plasma cells is not clear but may involve mitochondrial reprogramming.

Durable maintenance of Ag-specific Abs following secondary infection or booster immunization is desirable, so it is not clear why a ZBTB32-dependent genetic program exists to restrict such responses. One possibility is that only a finite number of long-lived plasma cells can be maintained because of limiting numbers of survival niches (55). An inability to properly attenuate secondary plasma cell responses could thus competitively antagonize pre-existing immunity over the course of a

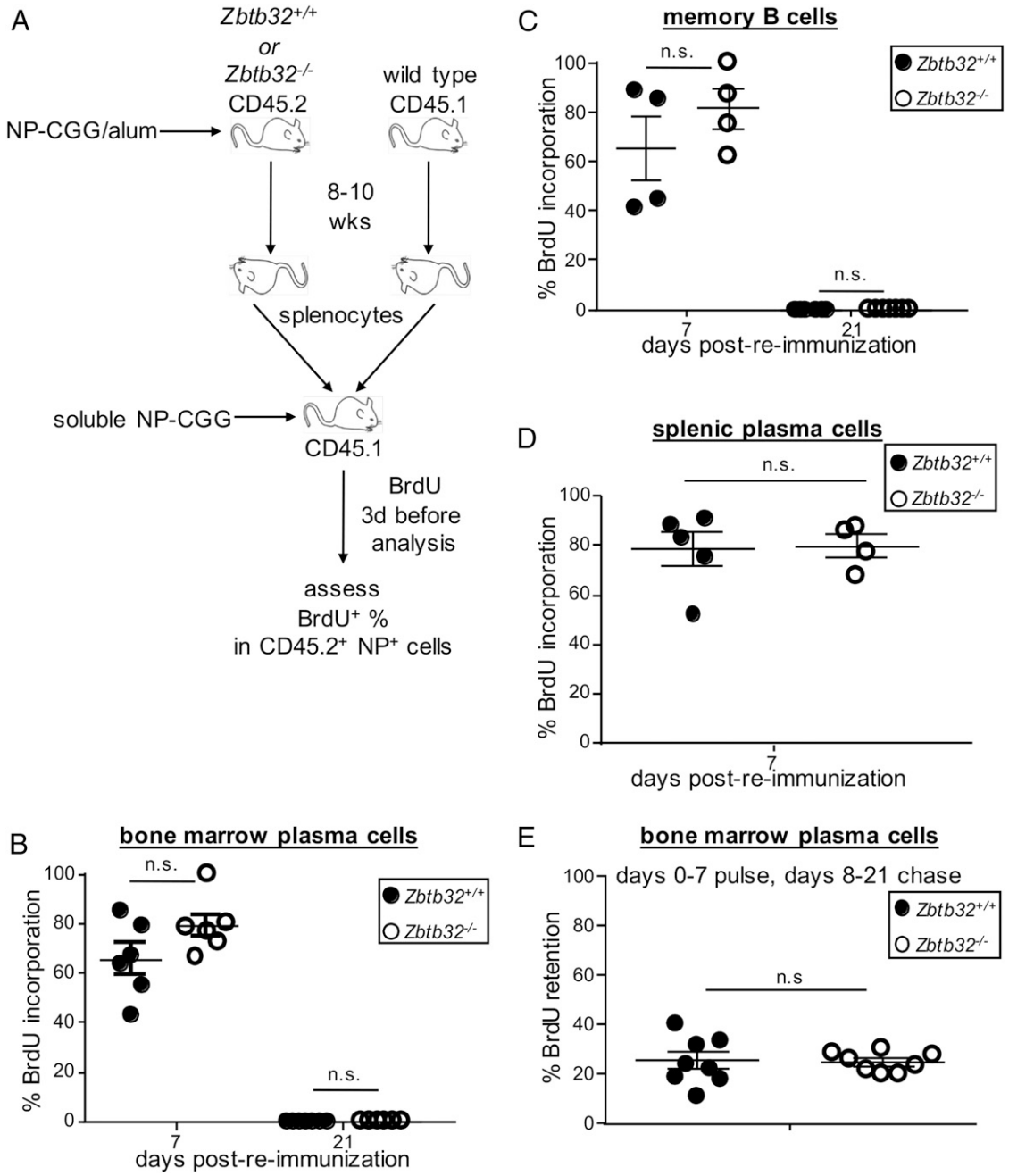

FIGURE 6. ZBTB32 deficiency promotes secondary plasma cell survival. (**A**) Schematic representation of the experimental setup. Percent BrdU incorporation in the donor CD45.2$^+$ NP–specific bone marrow plasma cells (**B**), memory B cells (**C**), and splenic plasma cells (**D**) at day 7 and day 21 post-rechallenge were quantified by flow cytometry. Statistical significance was calculated with an unpaired Student two-tailed *t* test. (**E**) Adoptive recipients were provided BrdU (2 mg/ml) in the drinking water for the first 7 d postimmunization and then given water with no BrdU for the next 14 d prior to euthanasia. Percent BrdU retention in donor CD45.2$^+$ bone marrow plasma cells is shown. Statistical significance was calculated with an unpaired Student two-tailed *t* test. Each panel represents cumulative data from two to five experiments.

lifetime (56). A second possibility is that in autoimmunity-susceptible backgrounds, ZBTB32 deficiency could exacerbate disease by prolonging autoantibody production. We did not observe any obvious signs of spontaneous autoimmunity in *Zbtb32*$^{-/-}$ mice, but they have been maintained in the largely resistant C57BL/6 strain. Finally, it is possible that ZBTB32 deficiency predisposes to B and plasma cell transformation and malignancy. Although not frequent, in the Multiple Myeloma Genomics Portal (https://www.broadinstitute.org/mmgp/home), we have identified at least one sample carrying a *Zbtb32* deletion. Moreover, the levels of ZBTB32 expression distinguish different types of diffuse large B cell lymphomas (57). Appropriate genetic models will help distinguish between these etiological possibilities.

Acknowledgments

We thank I-Cheng Ho for permission to use *Zbtb32*$^{-/-}$ mice. We also thank Krista Kennerly for laboratory management, You Zhou, Adrianus Boon, and Chyi Hsieh for technical assistance with experiments, Erica Lantelme and Dorian Brinja for assistance with flow cytometry, and Rachel Wong, Derrick Callahan, Wing Lam, and Hannah Pizzato for helpful comments on the manuscript.

Disclosures

The authors have no financial conflicts of interest.

References

1. Purtha, W. E., T. F. Tedder, S. Johnson, D. Bhattacharya, and M. S. Diamond. 2011. Memory B cells, but not long-lived plasma cells, possess antigen specificities for viral escape mutants. *J. Exp. Med.* 208: 2599–2606.
2. Manz, R. A., M. Löhning, G. Cassese, A. Thiel, and A. Radbruch. 1998. Survival of long-lived plasma cells is independent of antigen. *Int. Immunol.* 10: 1703–1711.
3. Slifka, M. K., R. Antia, J. K. Whitmire, and R. Ahmed. 1998. Humoral immunity due to long-lived plasma cells. *Immunity* 8: 363–372.
4. Glenny, A. T., and H. J. Südmersen. 1921. Notes on the production of immunity to diphtheria toxin. *J. Hyg. (Lond.)* 20: 176–220.
5. Pape, K. A., J. J. Taylor, R. W. Maul, P. J. Gearhart, and M. K. Jenkins. 2011. Different B cell populations mediate early and late memory during an endogenous immune response. *Science* 331: 1203–1207.
6. Martin, S. W., and C. C. Goodnow. 2002. Burst-enhancing role of the IgG membrane tail as a molecular determinant of memory. *Nat. Immunol.* 3: 182–188.
7. Engels, N., L. M. König, C. Heemann, J. Lutz, T. Tsubata, S. Griep, V. Schrader, and J. Wienands. 2009. Recruitment of the cytoplasmic adaptor Grb2 to surface IgG and IgE provides antigen receptor-intrinsic costimulation to class-switched B cells. *Nat. Immunol.* 10: 1018–1025.
8. Gitlin, A. D., L. von Boehmer, A. Gazumyan, Z. Shulman, T. Y. Oliveira, and M. C. Nussenzweig. 2016. Independent roles of switching and hypermutation in the development and persistence of B lymphocyte memory. *Immunity* 44: 769–781.
9. Waisman, A., M. Kraus, J. Seagal, S. Ghosh, D. Melamed, J. Song, Y. Sasaki, S. Classen, C. Lutz, F. Brombacher, et al. 2007. IgG1 B cell receptor signaling is inhibited by CD22 and promotes the development of B cells whose survival is less dependent on Ig α/β. *J. Exp. Med.* 204: 747–758.
10. Horikawa, K., S. W. Martin, S. L. Pogue, K. Silver, K. Peng, K. Takatsu, and C. C. Goodnow. 2007. Enhancement and suppression of signaling by the conserved tail of IgG memory-type B cell antigen receptors. *J. Exp. Med.* 204: 759–769.
11. Dogan, I., B. Bertocci, V. Vilmont, F. Delbos, J. Mégret, S. Storck, C. A. Reynaud, and J. C. Weill. 2009. Multiple layers of B cell memory with different effector functions. *Nat. Immunol.* 10: 1292–1299.
12. McHeyzer-Williams, L. J., P. J. Milpied, S. L. Okitsu, and M. G. McHeyzer-Williams. 2015. Class-switched memory B cells remodel BCRs within secondary germinal centers. *Nat. Immunol.* 16: 296–305.
13. Zuccarino-Catania, G. V., S. Sadanand, F. J. Weisel, M. M. Tomayko, H. Meng, S. H. Kleinstein, K. L. Good-Jacobson, and M. J. Shlomchik. 2014. CD80 and PD-L2 define functionally distinct memory B cell subsets that are independent of antibody isotype. *Nat. Immunol.* 15: 631–637.
14. Kometani, K., R. Nakagawa, R. Shinnakasu, T. Kaji, A. Rybouchkin, S. Moriyama, K. Furukawa, H. Koseki, T. Takemori, and T. Kurosaki. 2013. Repression of the transcription factor Bach2 contributes to predisposition of IgG1 memory B cells toward plasma cell differentiation. *Immunity* 39: 136–147.
15. Wrammert, J., D. Koutsonanos, G. M. Li, S. Edupuganti, J. Sui, M. Morrissey, M. McCausland, I. Skountzou, M. Hornig, W. I. Lipkin, et al. 2011. Broadly cross-reactive antibodies dominate the human B cell response against 2009 pandemic H1N1 influenza virus infection. [Published erratum appears in 2011 *J. Exp. Med.* 208: 411.] *J. Exp. Med.* 208: 181–193.
16. Klein, U., Y. Tu, G. A. Stolovitzky, J. L. Keller, J. Haddad, Jr., V. Miljkovic, G. Cattoretti, A. Califano, and R. Dalla-Favera. 2003. Transcriptional analysis of the B cell germinal center reaction. *Proc. Natl. Acad. Sci. USA* 100: 2639–2644.
17. Bhattacharya, D., M. T. Cheah, C. B. Franco, N. Hosen, C. L. Pin, W. C. Sha, and I. L. Weissman. 2007. Transcriptional profiling of antigen-dependent murine B cell differentiation and memory formation. *J. Immunol.* 179: 6808–6819.
18. Tomayko, M. M., S. M. Anderson, C. E. Brayton, S. Sadanand, N. C. Steinel, T. W. Behrens, and M. J. Shlomchik. 2008. Systematic comparison of gene expression between murine memory and naive B cells demonstrates that memory B cells have unique signaling capabilities. *J. Immunol.* 181: 27–38.
19. Wang, Y., and D. Bhattacharya. 2014. Adjuvant-specific regulation of long-term antibody responses by ZBTB20. *J. Exp. Med.* 211: 841–856.
20. Chevrier, S., D. Emslie, W. Shi, T. Kratina, C. Wellard, A. Karnowski, E. Erikci, G. K. Smyth, K. Chowdhury, D. Tarlinton, and L. M. Corcoran. 2014. The BTB-ZF transcription factor Zbtb20 is driven by Irf4 to promote plasma cell differentiation and longevity. *J. Exp. Med.* 211: 827–840.
21. Melnick, A., G. Carlile, K. F. Ahmad, C. L. Kiang, C. Corcoran, V. Bardwell, G. G. Prive, and J. D. Licht. 2002. Critical residues within the BTB domain of PLZF and Bcl-6 modulate interaction with corepressors. *Mol. Cell. Biol.* 22: 1804–1818.
22. Dent, A. L., A. L. Shaffer, X. Yu, D. Allman, and L. M. Staudt. 1997. Control of inflammation, cytokine expression, and germinal center formation by BCL-6. *Science* 276: 589–592.
23. Fukuda, T., T. Yoshida, S. Okada, M. Hatano, T. Miki, K. Ishibashi, S. Okabe, H. Koseki, S. Hirosawa, M. Taniguchi, et al. 1997. Disruption of the Bcl6 gene results in an impaired germinal center formation. *J. Exp. Med.* 186: 439–448.
24. Ye, B. H., G. Cattoretti, Q. Shen, J. Zhang, N. Hawe, R. de Waard, C. Leung, M. Nouri-Shirazi, A. Orazi, R. S. Chaganti, et al. 1997. The BCL-6 proto-oncogene controls germinal-centre formation and Th2-type inflammation. *Nat. Genet.* 16: 161–170.
25. Johnston, R. J., A. C. Poholek, D. DiToro, I. Yusuf, D. Eto, B. Barnett, A. L. Dent, J. Craft, and S. Crotty. 2009. Bcl6 and Blimp-1 are reciprocal and antagonistic regulators of T follicular helper cell differentiation. *Science* 325: 1006–1010.
26. Nurieva, R. I., Y. Chung, G. J. Martinez, X. O. Yang, S. Tanaka, T. D. Matskevitch, Y. H. Wang, and C. Dong. 2009. Bcl6 mediates the development of T follicular helper cells. *Science* 325: 1001–1005.
27. Yu, D., S. Rao, L. M. Tsai, S. K. Lee, Y. He, E. L. Sutcliffe, M. Srivastava, M. Linterman, L. Zheng, N. Simpson, et al. 2009. The transcriptional repressor Bcl-6 directs T follicular helper cell lineage commitment. *Immunity* 31: 457–468.
28. He, X., X. He, V. P. Dave, Y. Zhang, X. Hua, E. Nicolas, W. Xu, B. A. Roe, and D. J. Kappes. 2005. The zinc finger transcription factor Th-POK regulates CD4 versus CD8 T-cell lineage commitment. *Nature* 433: 826–833.
29. Sun, G., X. Liu, P. Mercado, S. R. Jenkinson, M. Kypriotou, L. Feigenbaum, P. Galéra, and R. Bosselut. 2005. The zinc finger protein cKrox directs CD4 lineage differentiation during intrathymic T cell positive selection. *Nat. Immunol.* 6: 373–381.
30. Savage, A. K., M. G. Constantinides, J. Han, D. Picard, E. Martin, B. Li, O. Lantz, and A. Bendelac. 2008. The transcription factor PLZF directs the effector program of the NKT cell lineage. *Immunity* 29: 391–403.
31. Kovalovsky, D., O. U. Uche, S. Eladad, R. M. Hobbs, W. Yi, E. Alonzo, K. Chua, M. Eidson, H. J. Kim, J. S. Im, et al. 2008. The BTB-zinc finger transcriptional regulator PLZF controls the development of invariant natural killer T cell effector functions. *Nat. Immunol.* 9: 1055–1064.
32. Lin, W., C. H. Lai, C. J. Tang, C. J. Huang, and T. K. Tang. 1999. Identification and gene structure of a novel human PLZF-related transcription factor gene, TZFP. *Biochem. Biophys. Res. Commun.* 264: 789–795.
33. Hoatlin, M. E., Y. Zhi, H. Ball, K. Silvey, A. Melnick, S. Stone, S. Arai, N. Hawe, G. Owen, A. Zelent, and J. D. Licht. 1999. A novel BTB/POZ transcriptional repressor protein interacts with the Fanconi anemia group C protein and PLZF. *Blood* 94: 3737–3747.
34. Miaw, S. C., A. Choi, E. Yu, H. Kishikawa, and I. C. Ho. 2000. ROG, repressor of GATA, regulates the expression of cytokine genes. *Immunity* 12: 323–333.
35. Beaulieu, A. M., C. L. Zawislak, T. Nakayama, and J. C. Sun. 2014. The transcription factor Zbtb32 controls the proliferative burst of virus-specific natural killer cells responding to infection. *Nat. Immunol.* 15: 546–553.
36. Kang, B. Y., S. C. Miaw, and I. C. Ho. 2005. ROG negatively regulates T-cell activation but is dispensable for Th-cell differentiation. *Mol. Cell. Biol.* 25: 554–562.
37. Piazza, F., J. A. Costoya, T. Merghoub, R. M. Hobbs, and P. P. Pandolfi. 2004. Disruption of PLZP in mice leads to increased T-lymphocyte proliferation, cytokine production, and altered hematopoietic stem cell homeostasis. *Mol. Cell. Biol.* 24: 10456–10469.
38. Yoon, H. S., C. D. Scharer, P. Majumder, C. W. Davis, R. Butler, W. Zinzow-Kramer, I. Skountzou, D. G. Koutsonanos, R. Ahmed, and J. M. Boss. 2012. ZBTB32 is an early repressor of the CIITA and MHC class II gene expression during B cell differentiation to plasma cells. *J. Immunol.* 189: 2393–2403.
39. Bortnick, A., I. Chernova, W. J. Quinn, III, M. Mugnier, M. P. Cancro, and D. Allman. 2012. Long-lived bone marrow plasma cells are induced early in response to T cell-independent or T cell-dependent antigens. *J. Immunol.* 188: 5389–5396.
40. McHeyzer-Williams, M. G., G. J. Nossal, and P. A. Lalor. 1991. Molecular characterization of single memory B cells. *Nature* 350: 502–505.
41. Kuraoka, M., A. G. Schmidt, T. Nojima, F. Feng, A. Watanabe, D. Kitamura, S. C. Harrison, T. B. Kepler, and G. Kelsoe. 2016. Complex antigens drive permissive clonal selection in germinal centers. *Immunity* 44: 542–552.
42. Tas, J. M., L. Mesin, G. Pasqual, S. Targ, J. T. Jacobsen, Y. M. Mano, C. S. Chen, J. C. Weill, C. A. Reynaud, E. P. Browne, et al. 2016. Visualizing antibody affinity maturation in germinal centers. *Science* 351: 1048–1054.
43. Honey, K., and A. Y. Rudensky. 2003. Lysosomal cysteine proteases regulate antigen presentation. *Nat. Rev. Immunol.* 3: 472–482.
44. Camps, M., A. Nichols, and S. Arkinstall. 2000. Dual specificity phosphatases: a gene family for control of MAP kinase function. *FASEB J.* 14: 6–16.
45. Leone, G., J. DeGregori, Z. Yan, L. Jakoi, S. Ishida, R. S. Williams, and J. R. Nevins. 1998. E2F3 activity is regulated during the cell cycle and is required for the induction of S phase. *Genes Dev.* 12: 2120–2130.
46. Bravo, R., R. Frank, P. A. Blundell, and H. Macdonald-Bravo. 1987. Cyclin/PCNA is the auxiliary protein of DNA polymerase-delta. *Nature* 326: 515–517.
47. Prelich, G., C. K. Tan, M. Kostura, M. B. Mathews, A. G. So, K. M. Downey, and B. Stillman. 1987. Functional identity of proliferating cell nuclear antigen and a DNA polymerase-delta auxiliary protein. *Nature* 326: 517–520.
48. Smits, P., J. Smeitink, and L. van den Heuvel. 2010. Mitochondrial translation and beyond: processes implicated in combined oxidative phosphorylation deficiencies. *J. Biomed. Biotechnol.* 2010737385.
49. Lam, W. Y., A. M. Becker, K. M. Kennerly, R. Wong, J. D. Curtis, E. M. Payne, K. S. McCommis, J. Fahrmann, H. A. Pizzato, R. M. Nunley, et al. 2016. Mitochondrial pyruvate import promotes long-term survival of antibody-secreting plasma cells. *Immunity.* 45: 1–14.
50. Weisel, F. J., G. V. Zuccarino-Catania, M. Chikina, and M. J. Shlomchik. 2016. A temporal switch in the germinal center determines differential output of memory B and plasma cells. *Immunity* 44: 116–130.
51. Tarlinton, D. 2006. B-cell memory: are subsets necessary? *Nat. Rev. Immunol.* 6: 785–790.
52. Amanna, I. J., and M. K. Slifka. 2010. Mechanisms that determine plasma cell lifespan and the duration of humoral immunity. *Immunol. Rev.* 236: 125–138.
53. Allen, C. D., T. Okada, H. L. Tang, and J. G. Cyster. 2007. Imaging of germinal center selection events during affinity maturation. *Science* 315: 528–531.

54. Victora, G. D., T. A. Schwickert, D. R. Fooksman, A. O. Kamphorst, M. Meyer-Hermann, M. L. Dustin, and M. C. Nussenzweig. 2010. Germinal center dynamics revealed by multiphoton microscopy with a photoactivatable fluorescent reporter. *Cell* 143: 592–605.
55. Moser, K., K. Tokoyoda, A. Radbruch, I. MacLennan, and R. A. Manz. 2006. Stromal niches, plasma cell differentiation and survival. *Curr. Opin. Immunol.* 18: 265–270.
56. Xiang, Z., A. J. Cutler, R. J. Brownlie, K. Fairfax, K. E. Lawlor, E. Severinson, E. U. Walker, R. A. Manz, D. M. Tarlinton, and K. G. Smith. 2007. FcγRIIb controls bone marrow plasma cell persistence and apoptosis. *Nat. Immunol.* 8: 419–429.
57. Care, M. A., S. Barrans, L. Worrillow, A. Jack, D. R. Westhead, and R. M. Tooze. 2013. A microarray platform-independent classification tool for cell of origin class allows comparative analysis of gene expression in diffuse large B-cell lymphoma. *PLoS One* 8: e55895.

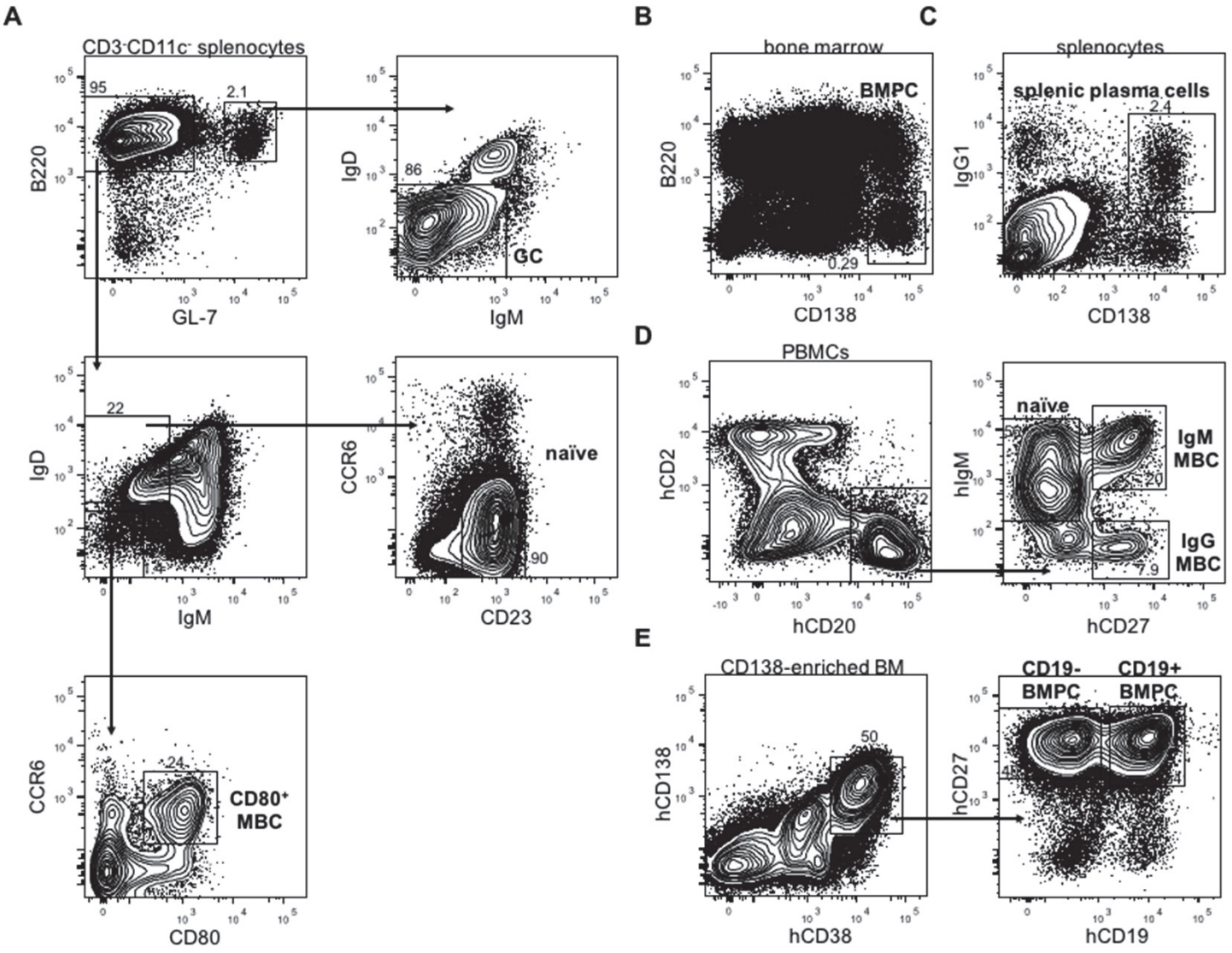

Supplemental Figure 1. Gating strategies for B cell subsets. Flow cytometry based identification and isolation of mouse (A-C) and human (D-E) B cell subsets. GC, germinal center B cells; MBC, memory B cells.

Supplemental Figure 2

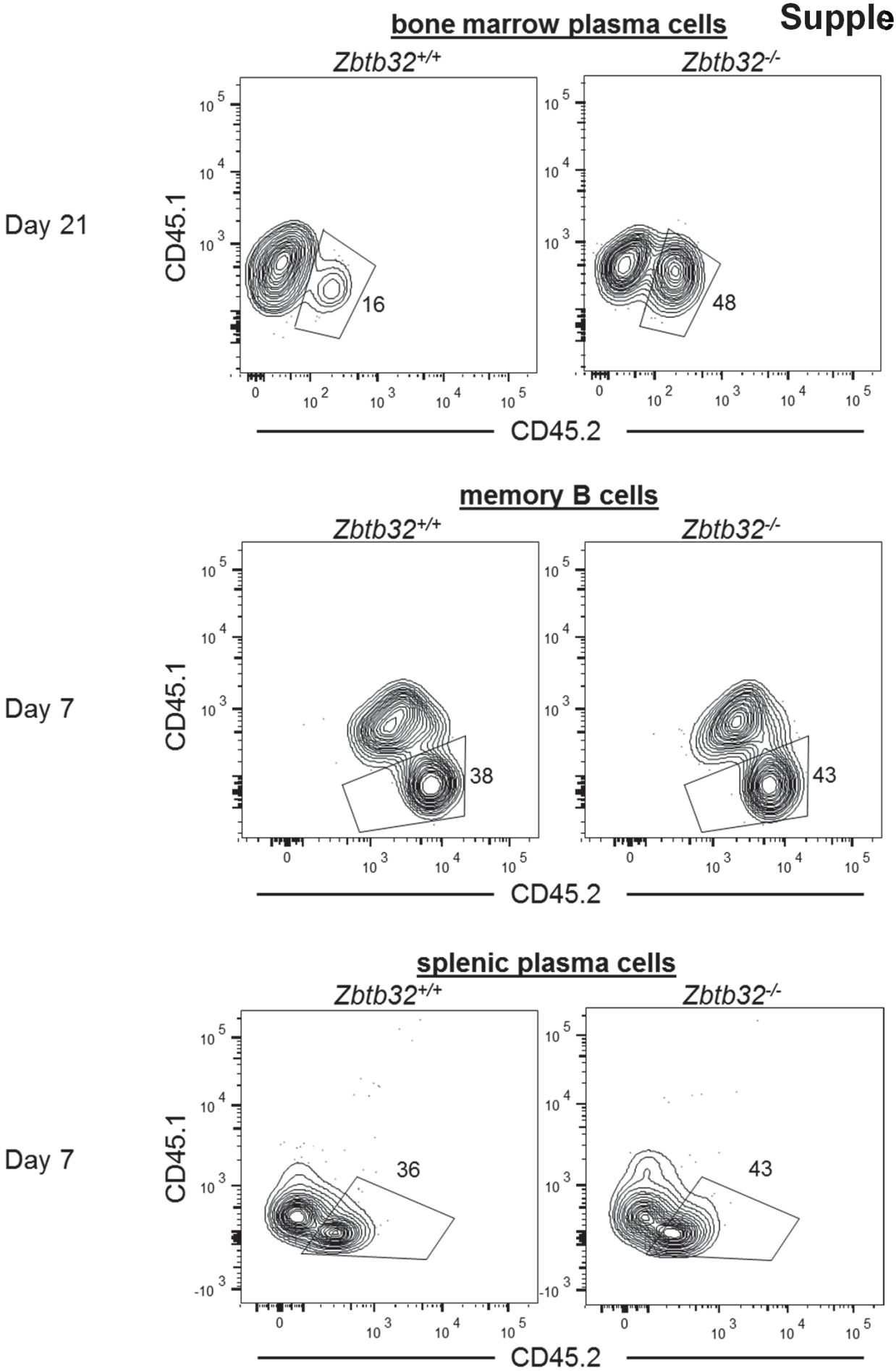

Supplemental Figure 2. Example plots for B cell chimerism shown in Figure 4.

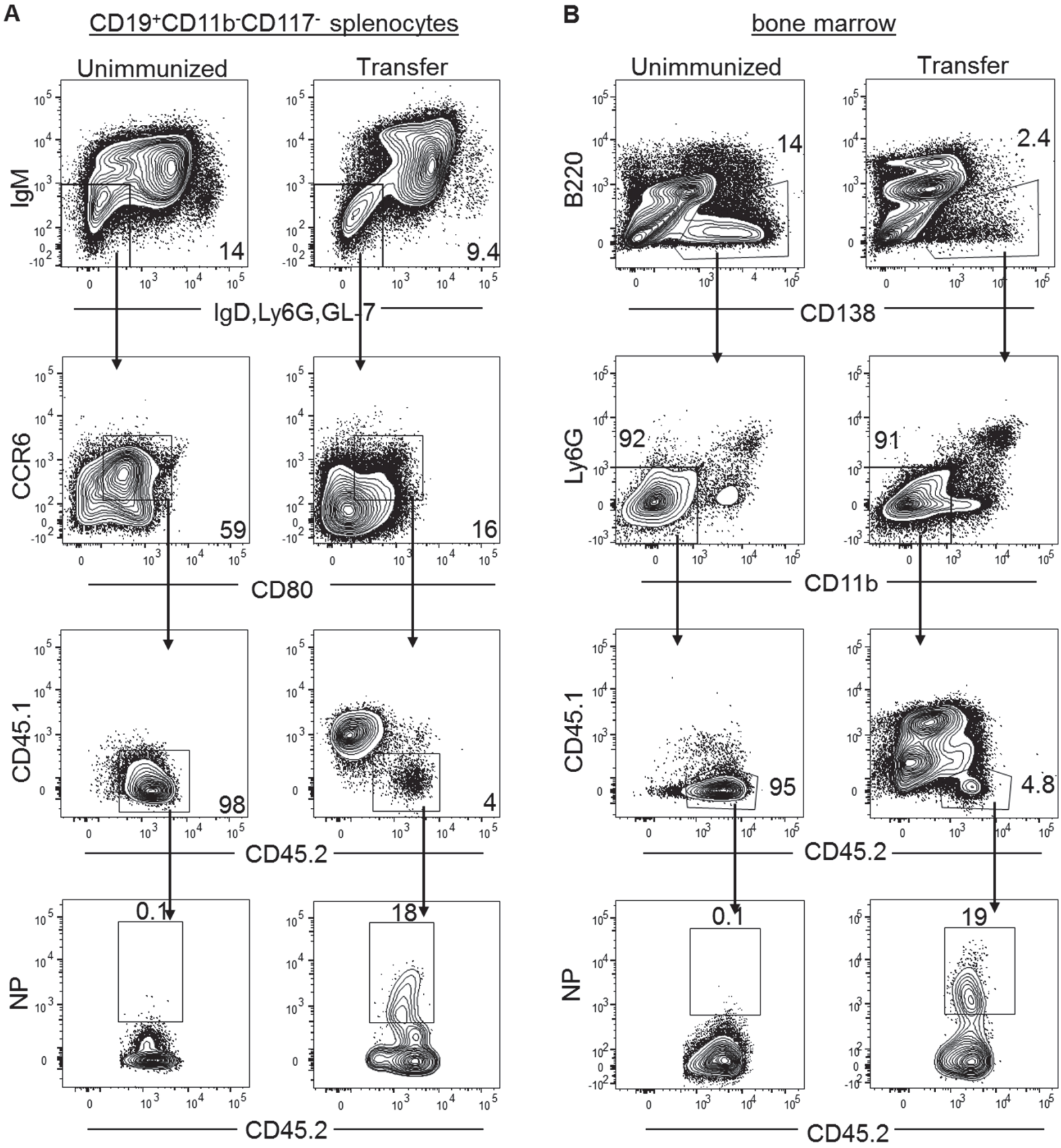

Supplemental Figure 3. Gating strategies for sorting NP specific donor (CD45.2) (A) memory B cells and (B) memory-derived bone marrow plasma cells

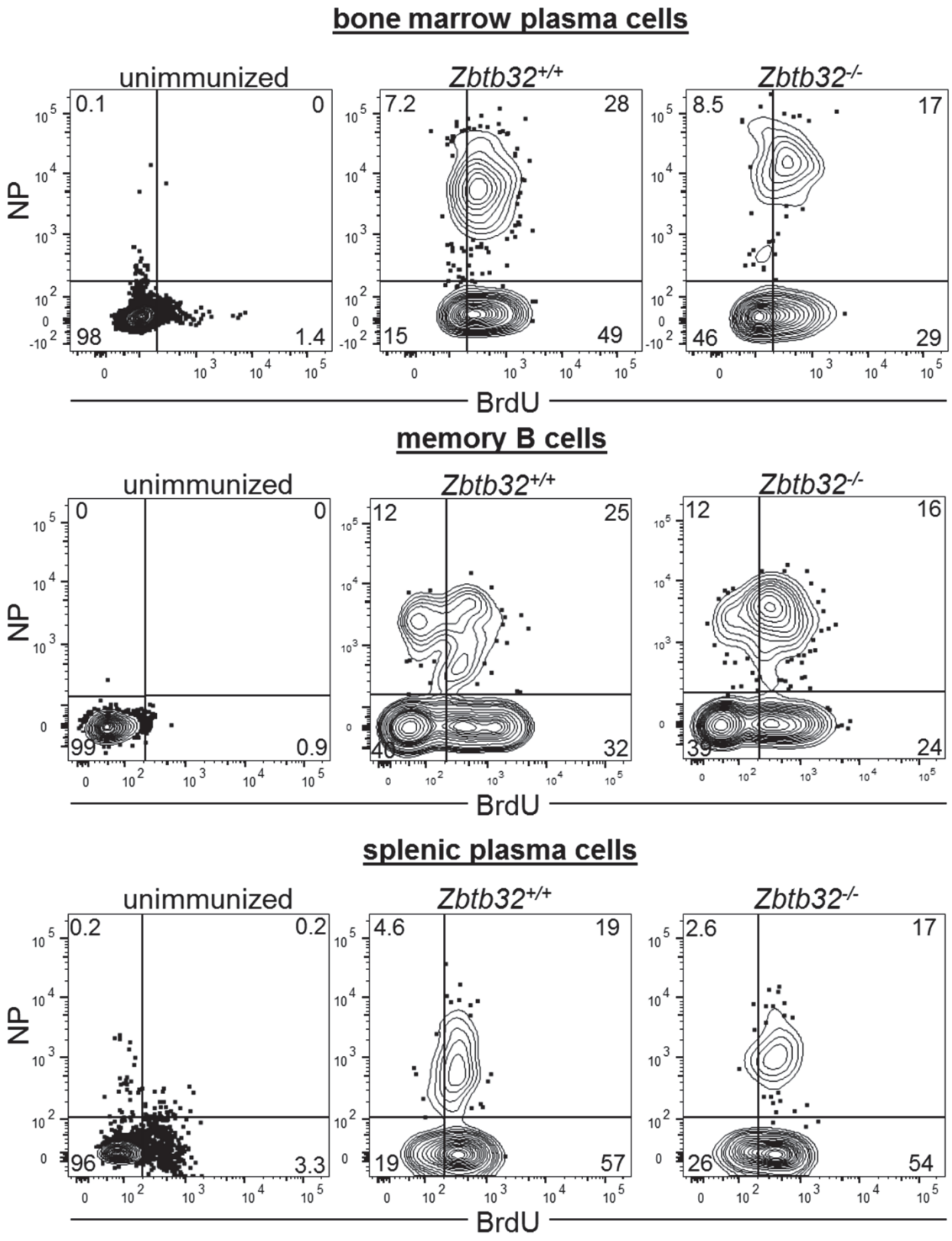

Supplemental Figure 4. Example plots for BrdU incorporation shown in Figure 6.